DESIGN OF THE DIAMOND LIGHT SOURCE DMM FOR THE VMXi BEAMLINE

D. J. Butler[†], J. H. Kelly, Diamond Light Source, Didcot, UK

Abstract

A Double Multilayer Monochromator (DMM) was designed in-house for the VMXi beamline. This paper describes the novel engineering solutions employed to build a high stability instrument. PiezoMotor® actuators drive sine-arm Bragg axes for both optics providing the coarse and fine motion in a single actuator. The long translation of the second multilayer is driven externally via a linear shift to eliminate in-vacuum pipe & cable motions. A high stability air bearing translates the whole DMM across the two multilayer stripes. The optics are water cooled via an Indium / Gallium eutectic alloy bath to minimise coupled vibrations. The DMM is operational on the VMXi beamline, experimental and performance data is presented.

INTRODUCTION

The in-situ Versatile Macromolecular crystallography (VMXi) beamline due to enter into service December 2016 is a high performance, high throughput autonomous upgrade to beamline I02. I02 currently operates a Double Crystal Monochromator (DCM) and the new DMM sits upstream of the DCM to allow both DCM and DMM based experiments. The DMM provides a broad energy band pass providing approximately 60x more photons to the sample. The overall design can be seen installed in the optics hutch (Fig. 1) and an isometric 3D CAD view (Fig. 2).
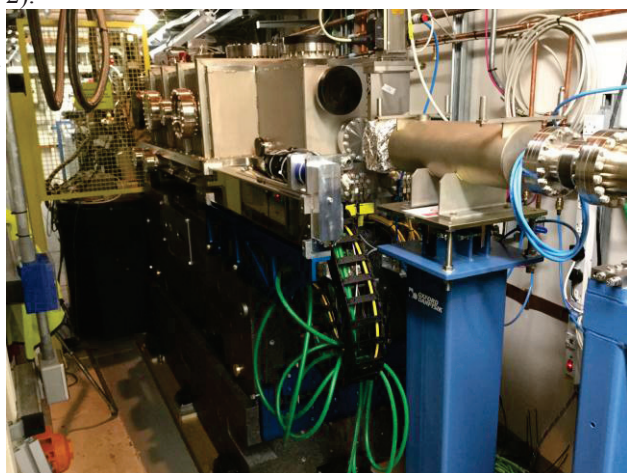

Figure 1: DMM installed in I02 optics cabin.

Stability of the beam was a critical criterion so throughout the design, care was taken to provide rigid mounting and stiff supports. Due to the shallow angles the DMM operates with, a relatively long travel in the beam axis is required. This is defined by the angular range and difference in multilayer heights. To maintain compatibility with the DCM, the DMM has a 25 mm vertical fixed

---

† d.butler@diamond.ac.uk

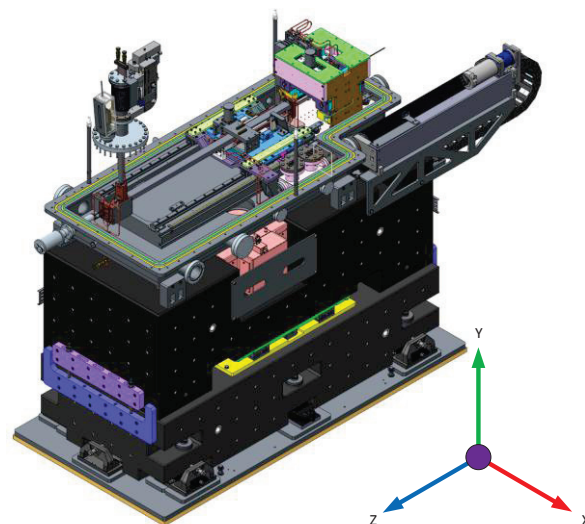offset so ML2 requires approximately 600 mm travel in the Z-direction (see Fig. 3).

Figure 2: 3D CAD model of the VMXi DMM.

This posed a number of design challenges to maintain pitch stability over this range (the DMM is largely insensitive to roll and yaw). From previous experience with commercial DMMs and DCMs it was decided that an in-house design would be developed. The storage ring at DLS currently operates at 300 mA but future upgrade to a Cryogenic Permanent Magnet Undulator (CPMU) would increase the ring current to 500 mA. The DMM has therefore been designed with this in mind. Table 1 details the specification and achieved performance.

Table 1: DMM Specification

Incident design power (CPMU @500mA)	~590 W
Incident beam size	3.4 x 2.1 mm (max)
Deflection Geometry	25 mm down
Energy Range	10-25 keV
Beam stability (measured)	34 nrad (RMS)

DMM COMPONENTS

At the heart of the design are the multilayers – a silicon substrate on which layers of heavy and light elements are deposited. The multilayer can therefore be produced with a prescribed d-spacing and the VMXi multilayer has 2x stripes at d-spaces of 2 nm and 2.4 nm. This allows an energy range between 10-25 keV with some energy overlap between the two multilayers. To select either multilayers the whole vessel is translated in the X-direction on a granite air bearing.
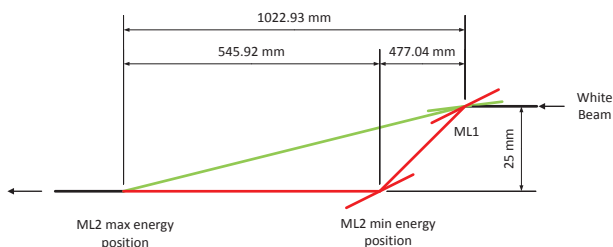
Figure 3: DMM optic geometry.

Multilayer Subassemblies

The two main subassemblies of the DMM are Multilayer 1 (ML1) and Multilayer 2 (ML2) which were designed to be assembled independently. This approach more favourably facilitated assembly, testing and commissioning at DLS. Each of the multilayer subassemblies sits on a cone, vee and 2x flats to increase stiffness while still providing repeatability in mounting. While not truly kinematic, due to the large span and relatively large mass the increased stability from 4x mounting points was preferred. The mount posts inside the vessel form a continuous solid path down to the granite and are coupled to the vessel via thin walled tubes. This allows some compliance without the need for bellows to isolate the internal components.

Multilayers

The silicon multilayers are shown in Fig. 4 with the two stripes clearly identified. ML1 (right hand multilayer) is upside down in this image. Both multilayers have troughs for cooling via an Indium-Gallium eutectic to reduce vibrations induced from the water chiller.
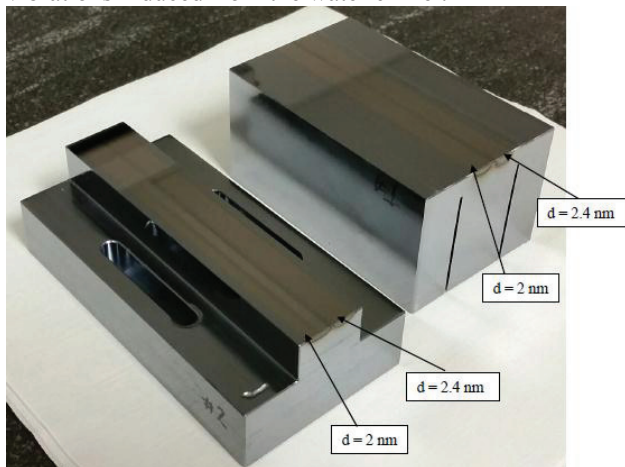

Figure 4: DMM Multilayers.

ML1 Assembly

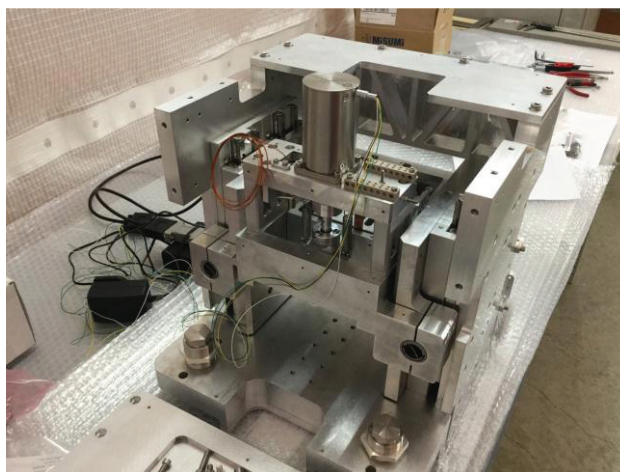ML1 subassembly is shown in Fig. 5 partially assembled and the 3D isometric view from CAD in Fig. 6.

Figure 5: ML1 subassembly partially assembled.
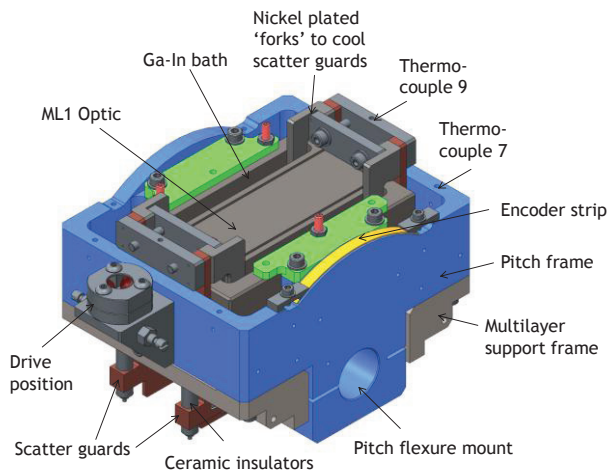
Bragg axis

Figure 6: ML1 multilayer pitch assembly.

ML1 pitch axis is driven via a linear PiezoMotor® actuator in a sine arm configuration. The hinge consists of Riverhawk crossed flexures to minimise free play and friction of the joint. The actuator is coupled via stainless (440C) balls in a nest of 3x ruby balls. This yields a high stiffness, compact and low friction joint that has a large angular range as required for the sine arm (see section view in Fig. 7).

Table 2: Bragg Axes Performance (ML1 & ML2)

Range	-0.5 to +1.5°
Resolution	< 0.1 µrad
Bidirectional repeatability	< 5 µrad
Accuracy	< 3 µrad / 8 mrad

Measurements in Diamonds Precision Metrology Lab for the pitch axis show good resolution, accuracy and repeatability (Table 2). Figure 8 details the results of a sweep with 5 count (71 nrad) steps demonstrating a very stiff structure. This shows that the system was able to meet and exceed the defined 0.5 µrad specification with negligible stick-slip in the crossed flexures and drive rod mechanism.
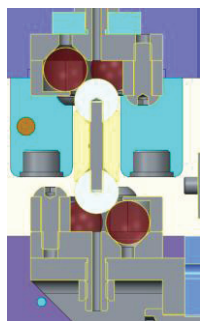
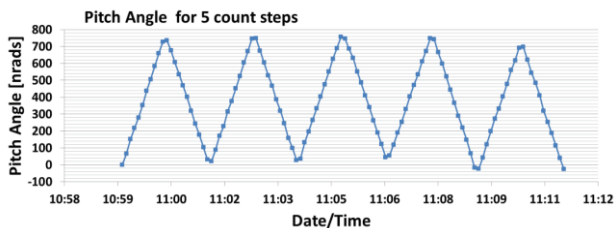Figure 7: Section of stainless ball on nest of ruby balls.

Figure 8: ML1 Bragg axis step scan measured with differential capacitive sensors [1].

Multilayer clamping and cooling To avoid distortion while still supporting the multilayer, a light preload was applied to push the multilayer against hardened stops. The optics are relatively insensitive to yaw so the horizontal stops were only positioned to standard manufacturing tolerances. The nominal roll and height however are more critical as ideally the Bragg axis would lie on the surface of the multilayer. 100TPI adjusters at 3x points on the lower surface were provided to support the multilayer and allow roll and height adjustment (Fig. 9).
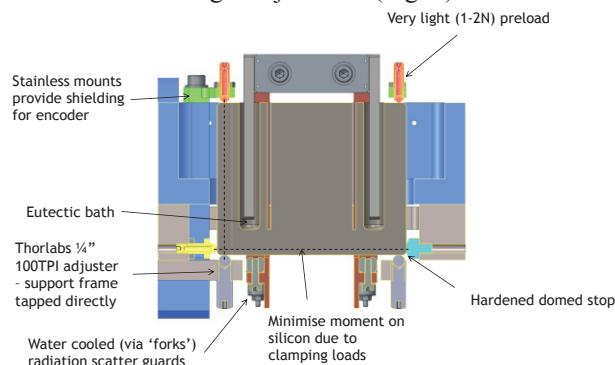

Figure 9: Section through ML1 substrate showing cooling and clamping method.

Roll axis and Y-axis To position ML1 on beam, vertical and roll axes are required. These two functions can be combined by making use of the differential position of the y-actuators. Riverhawk flexures were again utilised to provide the pin joints and a custom flexure was wire cut into the ML1 support frame to allow for the stretch of the assembly as the roll angle increased (see Figure 10).

Table 3: ML1 Y-axis Performance

Range	+5 mm – 7 mm
Resolution	0.25 µm
Bidirectional repeatability	1 µm over 0.7 mm
Parasitic pitch	50 µm over 0.7 mm

Table 4: ML1 (Virtual) Roll-axis Performance

Range	±1° (limited to ± 0.5°)
Resolution	1 µrad
Bidirectional repeatability	5.7 µrad
Parasitic pitch	175 µrad over 2°
Parasitic yaw	150 µrad over 2°

The vertical guidance for ML1 was achieved through 4x THK crossed roller tables (VRU-4205). Additional stiffness was harnessed by reducing the stroke to allow additional rollers in each bearing. This arrangement clearly leads to an over-constrained design so care was required when assembling to prevent binding. The result was an exceptionally stiff stage over the range with bidirectional repeatability measured as 0.2 µm over 0.7 mm range [2]. Table 3 and Table 4 detail the achieved specification of the Y and roll axes.

The vertical actuation for the ML1 y-axis was achieved through Huber Z-stages (5103.A10-X1) mounted on the granite outside of vacuum. These were coupled via slender flexure rods through bellows to exert a purely axial force on the assembly. The roll exhibited some nonlinearity (Fig. 11) due to the flexure that allows for the stretch in the frame. The overall roll error was found to be 5.7 µrad which was just outside of our 5 µrad spec but still acceptable.
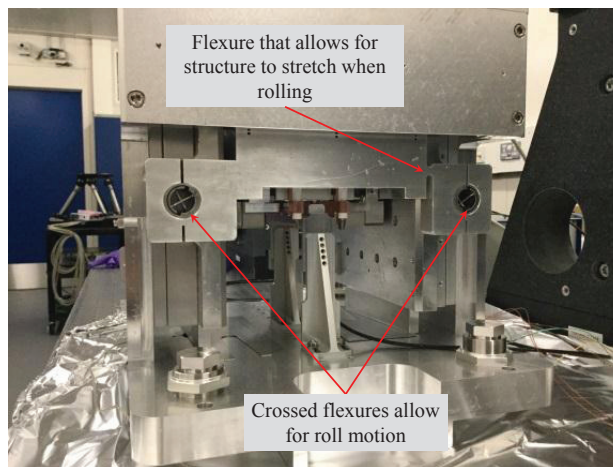

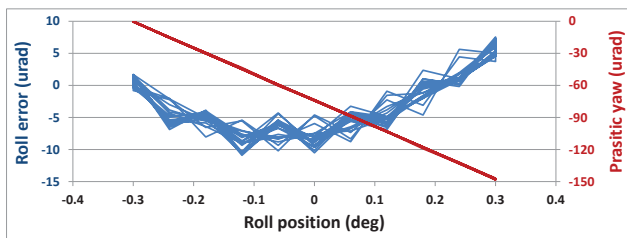Figure 10: ML1 assembly at Diamonds Precision Metrology Lab (PML) [2].

Figure 11: Parasitic pitch and yaw from roll axis [2].

ML2

The Bragg axis for ML2 is driven is the same manner as ML1 (i.e. Piezo actuator, sine arm driven through stainless on ruby spheres) so will not be discussed further.
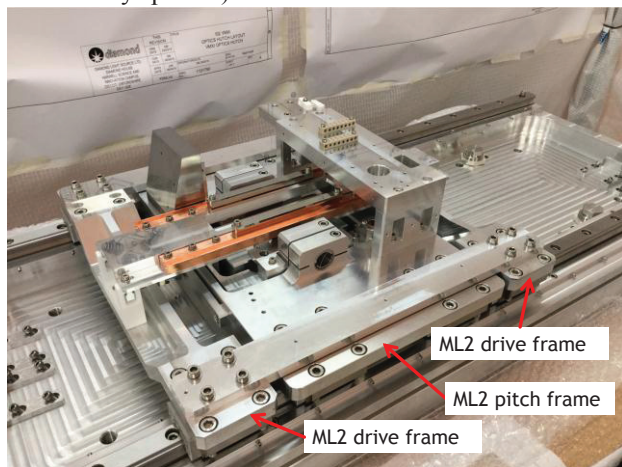

Figure 12: ML2 subassembly.

Z-axis   The Z-axis is driven via an external linear shift (UHV Design HLSML64, 600mm stroke) outside of vacuum mounted from a port on the vessel. Utilising a hollow shaft, the cables and cooling hoses were passed into the moving assembly. This results in no in-vacuum rolling cables that often cause issues as they move around. A re-entrant vessel was fixed to the end of the actuator and to allow for feedthroughs and cabling access. Figure 12 shows the 2nd multilayer assembly.

Table 5: ML2 Z-axis Performance

Range	580 mm
Resolution	2 μm
Bidirectional repeatability	64.8 μm (no vacuum loads)
Parasitic pitch	110 μrad
Parasitic yaw	20 μrad
Speed	100 mm/s

This approach however required the drive force to be off-axis (in the x-direction) so a yaw moment occurs as ML2 moves. The guidance for the Z-axis is through lightly preloaded THK HSR linear bearings. To reduce the yaw effect from the drive load the ML2 pitch frame is pushed through points on axis (balls on flats) via a drive frame on the same rails. It is this frame, not the ML2 pitch assembly which is driven by the actuator so any yaw

effects should be reacted by the frame and not the ML2 pitch assembly. Table 5 details the achieved performance.

Multilayer clamping and cooling   Similar to ML1, the aim was to lightly clamp the multilayer to avoid distortion holding the multilayer or from thermal effects. Direct access to the underside of the multilayer was impractical so a flexure based lever adjustment method was devised to allow roll and height adjustments from above (see Fig. 13).
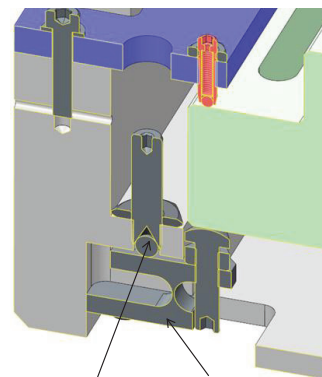

100 TPI adjuster   Lever flexure

Figure 13: ML2 flexure adjusters.

X-Axis

An actuator was developed to position and guide the vessel. A flexure based design provides vertical compliance for the 50μm lift of the air bearing while remaining stiff against yaw and pitch. The design is self-contained so was assembled, wired and tested in isolation to the rest of the DMM. Figure 14 shows the actuator installed and Table 6 details the achieved performance.

Table 6: X-axis Performance

Range	±15 mm
Bidirectional repeatability	4.5 μm
Parasitic pitch	5 μrad
Parasitic roll	8 μrad
Parasitic yaw	30 μrad

Figure 14: X-axis actuator and guidance for air bearing.

Shields, Masks and Thermal Issues

Scattered radiation causes drift of the beam position affecting stability as supports warm. Machine safety also required that the DMM could be interlocked with the

DCM to avoid sending DMM beam onto the DCM. A series of water cooled masks were designed to stop scattered radiation at 4x positions along the beam path:

i. A single slot front mask at beam height
ii. A mid mask between ML1 and ML2 with a large aperture for the swept beam
iii. A double slot end mask after ML2 that passes either through or the diverted DMM beam
iv. A combined beam position monitor (fluorescent screen), mask aperture and stop on a UHV linear shift to select position

Where possible, the beam path was enclosed with water cooled channels to catch scattering, heated components isolated and thermal paths minimised. Thermocouples were fitted to the assembly and show that the scatter guards around ML1 multilayer are warming. Over time this warms the ML1 pitch frame so a positional drift occurs. A future upgrade to cool the pitch and multilayer support frames is planned. It is currently not understood why this heating occurs but shows it was advantageous to enclose the beam path.

Vibration Stability

Seismometers were placed on the floor and ML2 assembly to measure the vibration amplification. Figure 15 and Fig. 16 show very low amplification factors of 1.05 in the vertical direction and 1.14 in the horizontal (Z) direction.
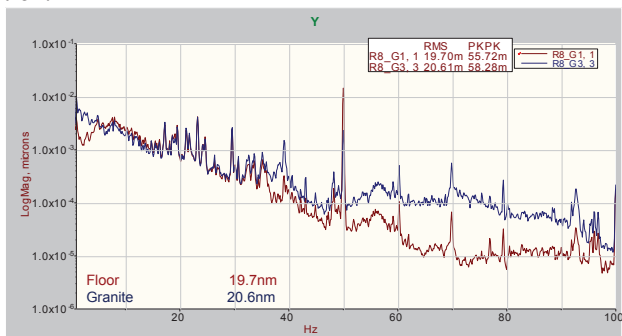

Figure 15: FFT of Vertical seismometer displacements of floor (red) and ML2 Frame (blue).
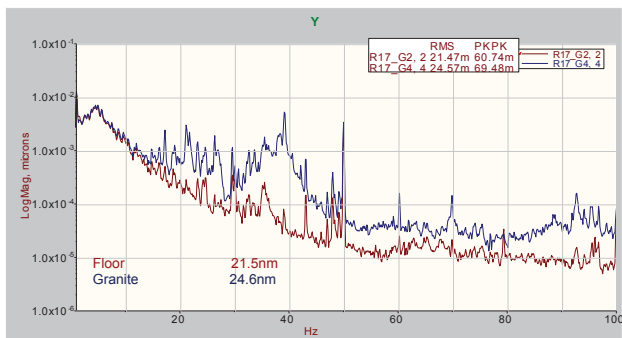

Figure 16: FFT of Horizontal seismometer displacements (Z-Direction) of floor (red) and ML2 Frame (blue).

BEAM STABILITY AT THE SAMPLE

The beam position was measured 13.5m downstream from ML1 using a 700Hz fast X-ray camera. Position

vibration of approximately 2.5µm pk-pk (Fig. 17) was measured and integrating over 1-350Hz (Fig. 18), the vibration amplitude of 34 nrad RMS was calculated. One of the largest sources of vibration in monochromatic instruments is typically the cooling fluid turbulence which is significantly exacerbated by the use of flexible hydroformed hoses. This DMM design provides a smooth bore fluid path and decouples the flexible rubber pipe sections from the optic supports.
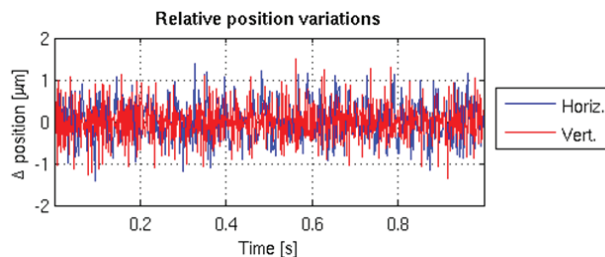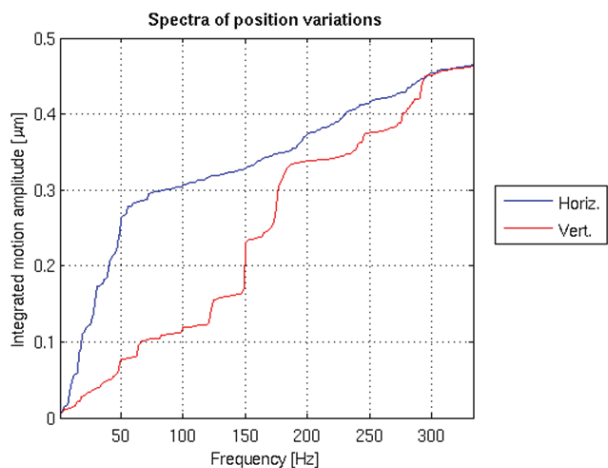

Figure 17: Beam vibration data.

Figure 18: Integrated (RMS) position from 1-350Hz.

CONCLUSIONS

The DMM for the VMXi Beamline was designed and developed in house and installed at the end of the December shutdown 2015. It has been in operation with users and a number of improvements identified. This paper has outlined a number of the innovations and demonstrated performance figures for the instrument.

ACKNOWLEDGEMENT

REFFERENCES

[1] Bugnar (2016), I02 DMM ML1 pitch motion and vibration metrology report, internal Diamond report

[2] Bugnar (2016), I02 DMM Metrology, internal Diamond report